

Role of electron-phonon interactions and external strain on the electronic properties of semiconducting carbon nanotubes

D. Karauskaj* and A. Mascarenhas

National Renewable Energy Laboratory, 1617 Cole Boulevard, Golden, Colorado 80401-3393, USA

(Received 22 May 2006; published 28 March 2007)

The electron-phonon interactions determine the temperature dependent photoluminescence of semiconducting carbon nanotubes. Both effects, the energy shifts and spectral narrowing of the transitions, can be attributed to the electron-phonon interaction. In this paper, we present an accurate measurement of the temperature induced broadening of the photoluminescence transitions of carbon nanotubes, and model this broadening in terms of the theory, previously used to model the thermal broadening of critical points in conventional semiconductors. Through this fitting procedure, parameters could be estimated which provide important insight into the strength of the electron-phonon interactions. Moreover, careful studies of the energy shifts induced by the external strain had revealed a $n-m$ family behavior. We further conclude that using a mathematical expression that combines the theory of semiconducting carbon nanotubes under hydrostatic pressure and strain, this family behavior observed experimentally could be theoretically reproduced, providing tools to model and predict the effect of strain on the electronic properties of carbon nanotubes.

DOI: [10.1103/PhysRevB.75.115426](https://doi.org/10.1103/PhysRevB.75.115426)

PACS number(s): 73.22.-f, 78.67.Ch, 63.22.+m

I. INTRODUCTION

The many-particle interactions play an important role in determining the electronic properties of semiconducting nanotubes and it has now become clear that many-body interactions, such as excitonic,^{1,2} electron-electron,³ and electron-phonon interactions,^{4,5} play an important role in determining the optical transition energies. The electron-phonon coupling in carbon nanotubes has been intensively investigated in relation with transport phenomena,^{6,7} resonance Raman excitation spectra,^{8,9} excited-state carrier lifetimes,¹⁰ and excitonic effects.^{5,11} The effect of temperature on the photoluminescence (PL) electronic band gap E_g of carbon nanotubes has an enormous importance in determining the role of the electron-phonon interactions.^{4,12,13} The difficulty in experimentally determining the temperature behavior of the optical transitions of nanotubes lies in the surrounding environment. The encapsulation by the surfactant avoids bundling and makes the PL of the nanotubes possible. However, cooling the suspension below the freezing point can lead to strain effects, and heating it can remove the surfactant molecules and lead to energy shifts due to rebundling. The first studies of the temperature dependence of carbon nanotubes grown on silicon pillars have provided important insight into their temperature behavior¹⁴ and the effect of different inert gases on their emission.¹⁵ Other experiments have examined the effect of strain induced by the surrounding environment at low temperatures and the effect of hydrostatic pressure on the band gap of carbon nanotubes.^{16,17} In this paper, we carefully examine the temperature behavior of the band gap in terms of the spectral broadening of the transitions caused by the electron-phonon interaction. These effects can be well fitted by a theoretical approach successfully used in conventional semiconductors. We further examine the extrinsic effect of strain on the electronic properties of carbon nanotubes, induced by the polymer encapsulation. By combining the calculations on the effect of strain¹⁸ with recent calculations on the effect of hydrostatic pressure on the

electronic properties of semiconducting carbon nanotubes,^{19,20} we successfully reproduced the energy shift of the photoluminescence transitions with strain including the observed $n-m$ family behavior.

II. SAMPLES AND EXPERIMENT

Using a method similar to the one previously reported in Ref. 22, the as-produced high-pressure CO conversion single-walled carbon nanotubes (SWNTs) (Carbon Nanotechnologies) were suspended in aqueous (D_2O) sodium dodecyl sulfate (SDS). In order to lower the freezing temperature, the aqueous suspension of SWNTs was mixed with glycerol (1:2 v/v). A second solution mixture was prepared using a different surfactant, namely, dodecylbenzenesulfonic acid (DDBS). An aliquot of the DDBS surfactant stabilized SWNTs was added to an Eastman AQ55 polymer solution (Eastman Chemical Company). The mixture was stirred and lyophilized, resulting in a gray SWNT-AQ55 powder. The solution mixture or the polymer powder containing the nanotubes was mounted inside a variable temperature cryostat. The PL spectra were recorded using a grating spectrometer, equipped with a liquid-nitrogen-cooled InGaAs array detector. Several excitation energies were used, starting with 730 nm from a tunable continuous-wave Ti:sapphire laser and 590 and 650 nm from tunable dye lasers. In order to identify the nanotube species present in the solution and the polymer, room-temperature PL excitation (PLE) spectra were taken.²¹ The PLE maps were collected using a tunable excitation source, a broadband tungsten lamp dispersed in a grating spectrometer, and the PL was detected using a Fourier transform infrared spectrometer, equipped with a liquid-nitrogen-cooled germanium detector. The PLE spectra looked very similar in both the solution and the polymer. An energy shift was observed for the nanotube species between the two environments, most likely due to the change of the surrounding dielectric constant. The PLE maps revealed the excitation wavelengths needed to resonantly excite most of

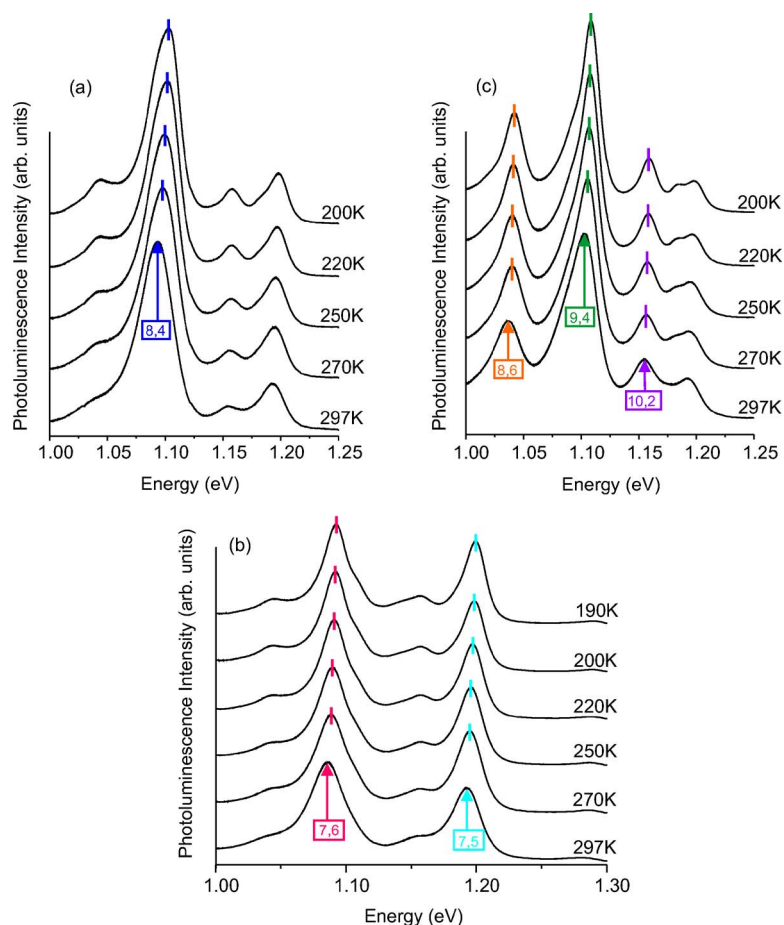


FIG. 1. (Color online) Photoluminescence spectra of the carbon nanotubes in SDS solution mixture for different temperatures in the strain-free region from 190 to 297 K resonantly excited with the (a) 590 nm, (b) 650 nm, and (c) 730 nm source with the E_{22} transition of the labeled nanotube species. The carbon nanotube species have been identified using the PLE spectra as described in Ref. 21. A small blueshift of the peak energies with decreasing temperature can be observed, indicated by the vertical colored ticks.

the nanotube species in order to increase their emission efficiency and avoid off-resonance effects.

III. EXPERIMENTAL RESULT

The PL spectra from the SDS nanotube solution mixture with glycerol were recorded starting at 297 K, and gradually cooling down to liquid-helium temperature of 4.2 K. The temperature change led to energy shifts of the transition lines and reduction in emission linewidths. While decreasing the temperature between 297 and 190 K, we observed small blueshifts in the PL emission lines, which were slightly different for different carbon nanotube species, and were reproducible after cooling down to 4.2 K and heating the solution back to room temperature. After decreasing the temperature below critical point where strain from the ice matrix occurs, an abrupt shift in the PL energies was observed.¹² Below the critical temperature which appears to be between 160 and 190 K, the PL from the (7,5) species belonging to the $\nu=(n-m)\bmod 3=2$ family shifts more strongly to higher energy with decreasing temperature, whereas for the (7,6) species, belonging to the $\nu=1$ family, the shift reverses direction. This opposite shift of the two families has been attributed to the effect of strain on the nanotubes,^{16,18,19,23,24} and the contraction induced by the ice phase transition could lead to external strain. The fact that no strain effect was observed at temperatures above 190 K led us to the conclusion that the energy shifts are most likely due to the shift of

the electronic band gap with temperature. The PL spectra of carbon nanotubes in the SDS solution mixture for different temperatures are shown in Fig. 1. In the strain-free region between 190 and 297 K, the solution was resonantly excited with the 590 nm source [Fig. 1(a)], 650 nm source [1(b)], and 730 nm source [Fig. 1(c)] with the E_{22} transition of the labeled nanotube species. The carbon nanotube species have been identified using the PLE spectra as described in Ref. 21. The unlabeled peaks in Fig. 1 originate from carbon nanotubes; however, only the resonantly excited peaks have been labeled. A small blueshift of the peak energies with decreasing temperature can be observed for all species, as indicated by the vertical colored ticks. The surfactant molecules surrounding the nanotubes are a possible source that could influence the observed energy shifts and linewidths of the emission lines. The change of the dielectric constant with temperatures could, for example, induce energy shifts. In order to exclude such effects, originating from the surfactant molecules contacting the nanotube, a second solution with a different surfactant, namely, DDBS, was mixed with glycerol and was studied under the same conditions. The PL spectra of the carbon nanotubes in SDS and DDBS solution mixture for different temperatures from 200 to 297 K and resonantly excited with the 650 nm source with the E_{22} transition of the (7,6) and (7,5) species are shown, respectively, in Figs. 2(a) and 2(b). The vertical lines indicate the energy positions of the (7,6) and (7,5) nanotube species at 200 and 297 K in the two solution glycerol mixtures with different surfactants.

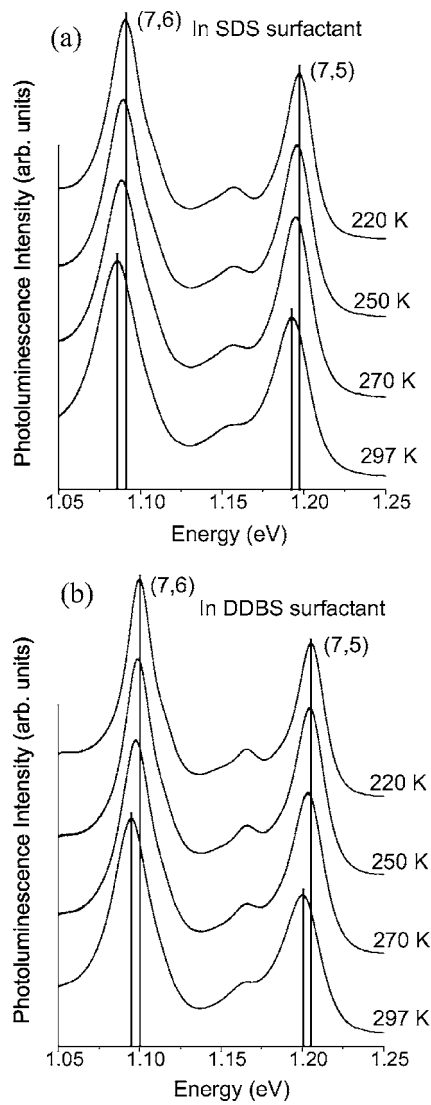


FIG. 2. Photoluminescence spectra of the carbon nanotubes in (a) SDS and (b) DDBS solution mixture for different temperatures from 200 to 297 K resonantly excited with the 650 nm source with the E_{22} transition of the (7,6) and (7,5) species. The vertical lines indicate the energy positions of the (7,6) and (7,5) nanotube species at 200 and 297 K in the two solution glycerol mixtures with different surfactants. A constant energy shift of the transition lines can be observed, as a result of the change of the dielectric constant of the surrounding environment. However, the relative energy shifts with temperature are identical for both solution mixtures prepared using different surfactants.

There is a constant energy shift in the emission lines due to the change of the dielectric constant of the surrounding surfactant, but the relative energy shifts with temperature were identical. Therefore, it appears that up to the freezing point of the solution, the environment does not affect the temperature behavior of the emission of the nanotubes.

After having concluded that effects originating from the surrounding environment are unlikely, we proceed with the first central observation of this paper. Besides the energy shifts, a substantial narrowing of the linewidths with decreasing temperature could be observed that most surprisingly

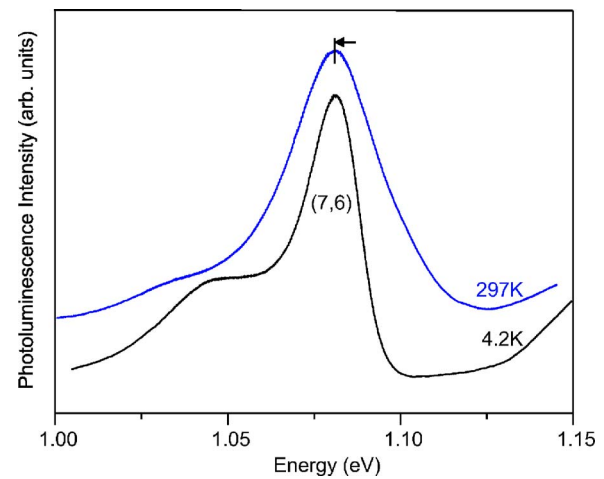


FIG. 3. (Color online) Photoluminescence spectra of the (7,6) carbon nanotube species in SDS solution mixture at 4.2 and 297 K, excited with the 650 nm source. The horizontal black arrow indicates the amount of the spectrum at 4.2 K that has been redshifted in order to compare the two spectra. A substantial reduction of the linewidth with decreasing temperature can be observed. The full width at half maximum of the (7,6) nanotube species of 30.5 meV at 297 K is reduced to 20.6 meV at 4.2 K.

persists beyond the ice phase transition of the solution all the way to 4.2 K. The largest line narrowing at low temperature is observed for the (7,6) tube. The full width at half maximum of 30.5 meV at 297 K is reduced to 20.6 meV at 4.2 K. This behavior persists beyond the critical temperature where strain occurs, which indicates a uniformly induced strain by the ice matrix, since random strains have the opposite effect leading to line broadening. The PL spectra of the (7,6) carbon nanotube species at 4.2 and 297 K are shown in Fig. 3. The horizontal black arrow indicates the amount of the spectrum at 4.2 K that has been redshifted in order to compare the two spectra. The full width at half maximum (FWHM) obtained by a simple multiline Voigtian fit has been plotted in Fig. 4 as a function of temperature in the strain-free region for several carbon nanotube species. A monotonic reduction in the FWHM can be observed for all nanotubes. However, for certain tubes the linewidth reduction is larger than for others, most likely due to the chirality and/or diameter dependence of the electron-phonon coupling in semiconducting carbon nanotubes. The temperature dependence of the band gap of conventional semiconductors at constant pressure can be separated into harmonic and anharmonic contributions: $(\partial E_g / \partial T) = (\partial E_g / \partial T)_{har} + (\partial E_g / \partial T)_{anhar}$. The harmonic term arises from the electron-phonon interaction, while the anharmonic term is due to the thermal expansion.^{25,26} The contribution from the thermal expansion is smaller and can be neglected in the first approximation. The temperature dependence of the band gap can be obtained to first approximation by evaluating the harmonic term. The renormalization of the unperturbed electron energy E_k^o with wave vector \vec{k} by the electron-phonon interaction can be written as

$$E_k = E_k^o + \Delta_k^{DW} + \Delta_k^{SE} + i\Gamma_k, \quad (1)$$

where Δ_k^{DW} is the energy shift induced by the ‘‘Debye-Waller’’ term. The complex ‘‘self-energy’’ term has a real part

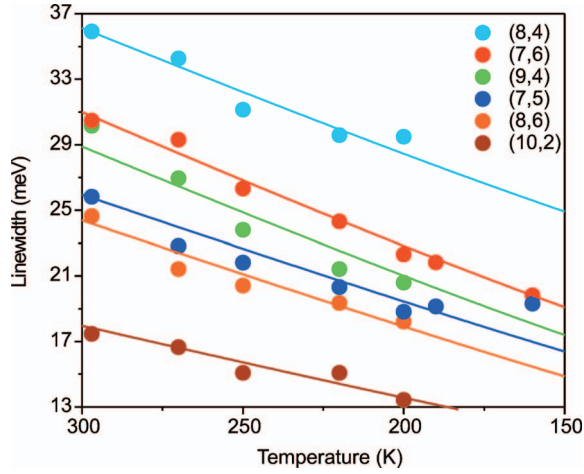


FIG. 4. (Color) Full width at half maximum of the transition lines of six carbon nanotube species as a function of decreasing temperature. A substantial reduction in linewidth with decreasing temperature in the strain-free region between 200 and 297 K can be observed.

Δ_k^{SE} , leading to an energy shift of the electronic states, and an imaginary part Γ_k , which causes a lifetime broadening of the electronic states.^{27–29} The evaluation of the harmonic term including both the self-energy and Debye-Waller contributions is quite challenging; therefore, approximate models have shown to be very useful tools in the evaluation of the temperature dependence of the band gap of solids.²⁹ In order to reproduce the energy shifts with temperature, we previously used an approximate model for E_g of semiconducting SWNTs in the temperature range of $T < 400$ K based on a two-phonon model introduced by Viña *et al.*²⁹ and successfully adopted to carbon nanotubes in Ref. 4 such that the parameters include diameter and chirality effects. This model provided an excellent fit to the simulations obtained by fully evaluating the harmonic term, and the fitting parameters were listed. The magnitude of the observed shifts was larger than the previously reported values^{15,30} and only a moderate chirality and/or diameter dependence was observed.¹² The observed temperature dependence of the linewidths origi-

TABLE I. Values for the inhomogeneous broadening Γ_I and effective electron-phonon coupling Γ_0 used in the fitting process of the linewidths of the photoluminescence transitions with $E_\Theta = 34.5$ meV, and the values for $\Gamma_0^* = \alpha_2 \Theta_2$ used in Ref. 12 to reproduce the energy shift of the band gap with temperature, where α_2 and Θ_2 are defined in Ref. 4.

SWCN	Γ_I (meV)	Γ_0 (meV)	Γ_0^* (meV)
(8,4)	17.1	16.3	12.5
(7,6)	11.1	18.7	17.2
(9,4)	9.5	17.2	11.2
(7,5)	9.0	10.5	16.5
(8,6)	7.5	10.3	14.8
(10,2) ^a	6.9	8.7	8.3

^aA scattering rate $\alpha = 26.5 \mu\text{eV/K}$ was used for this nanotube.

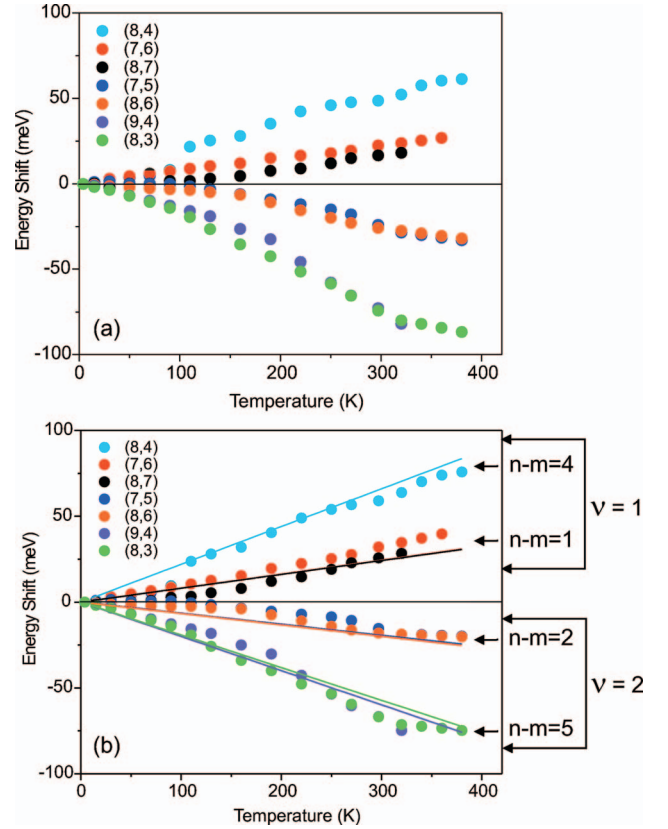


FIG. 5. (Color) Energy shift of the carbon nanotube species with temperature. The behavior of the two nanotube families, $\nu=1$ and 2, indicates strain induced by the wrapping polymer. In (a) the experimental line positions prior to removing the temperature dependence are shown, whereas in (b) the temperature shift of the band gap has been subtracted. The lines show the best fits to the experimental data using Eq. (3).

nates from the homogeneous broadening due to electron-phonon interactions. If the change in the line broadening can be entirely assigned to the intrinsic properties of the nanotubes, i.e., vibrational energy transfer from the D₂O surfactant solution can be neglected, by fitting the temperature dependence important parameters can be obtained, such as the effective electron-phonon coupling. The electron-phonon interaction is of enormous importance to the optical and transport properties of SWNTs, and has been a subject of numerous theoretical studies.^{8,9,31–36} In order to reproduce the thermal broadening of the emission lines of carbon nanotubes, we use an approximate model introduced in Refs. 37–42 and successfully applied to reproduce the thermal broadening of the excitonic emission lines in semiconducting quantum wells and quantum wires. The expression used to fit the temperature dependence of the emission lines of SWCNTs similarly contains a linear exciton phonon scattering term and a term originating from the coupling to an average phonon proportional to the phonon population:

$$\Gamma(T) = \gamma + \alpha T + \Gamma_I + \frac{\Gamma_0}{e^{E_\Theta/kT} - 1}, \quad (2)$$

where γ_0 is the lifetime broadening which has been omitted here, Γ_I is the temperature independent inhomogeneous

broadening, α is the exciton phonon scattering rate, Γ_0 is the effective electron-phonon coupling, and $E_\Theta = 34.5$ meV is an average phonon energy. In semiconducting quantum wells and wires, the interaction with acoustic phonons induced by the deformation potential and piezoelectric scattering mechanism leads to the linear term in the emission linewidth and dominates at lower temperatures, whereas the Fröhlich coupling with the longitudinal-optical phonon is described by a term proportional to the phonon population and dominates the thermal broadening of the emission lines at higher temperatures. Although the electron-phonon interaction mechanisms are different, this model reproduces the temperature dependence of the broadening of the excitonic lines in SWNTs. A scattering rate α as high as $12 \mu\text{eV/K}$ was measured for a 29 nm wire width and a rapid increase of α with decreasing wire width was observed.⁴² For the substantially narrower SWNTs, a scattering rate of $44 \mu\text{eV/K}$ was estimated and used in the fit shown in Fig. 4. The electron-acoustic-phonon scattering has been shown to be significant in the transport properties of SWNTs.⁴³ Possible diameter and/or chirality variations of the scattering rate between nanotube species were neglected. The electron-phonon coupling Γ_0 and the inhomogeneous broadening Γ_I were varied to obtain the best fit. The values for Γ_0 and Γ_I obtained for the nanotubes are listed in Table I. The inhomogeneous broadening obtained by the fitting procedure is in well agreement with single nanotube studies, which report a distribution of emission energies of about ~ 10 meV.^{30,44} The values for the electron-phonon coupling Γ_0 obtained by the fitting procedure are similar to the $\Gamma_0^* = \alpha_2 \Theta_2$ obtained from the energy shifts of the band gap^{4,12} and are listed in Table I. Contributions from other nanotube species increase the difficulty in determining the linewidth. Nevertheless, the values for Γ_0 listed in Table I show a level of consistency, despite some variation, due most likely to some intrinsic diameter and/or chirality dependency.

We further examine the effect of external strain on the electronic properties of carbon nanotubes, which occurs while changing the temperature of the polymer wrapped semiconducting carbon nanotubes. The spectra were collected in the temperature range of 1.8–380 K and show significantly larger temperature shifts than the previous ones, indicating a different mechanism. The energy shifts of the different species with temperature have been plotted in Fig. 5, where the low-temperature end has been chosen as a reference. In order to be able to plot all species together and to highlight the behavior of each species, the low-temperature (1.8 or 4.2 K) energy position has been subtracted and the energy shifts have been plotted as a function of increasing temperature. Different behaviors can be observed for the two nanotube $\nu=1$ and $\nu=2$ families, similar to the behavior observed in the SDS suspension below the critical temperature, which is mostly due to external strain that discriminates between the two nanotube families,^{18,19,23,24} and unavoidably to a lesser amount, due to the intrinsic change of the band gap with temperature. We used previous results^{4,12} in order to subtract the temperature dependence and obtain the pure strain behavior. The experimental data together with the best fits are shown in Fig. 5(b). In Fig. 5(a), we show the energy shifts of the peak positions prior to removing the temperature

dependence of the band gap for comparison. After removing the temperature dependence of the band gap, the nanotube species are distributed symmetrically around the reference point (0 meV) as predicted by theory^{18,19,23} and approach the expected linear behavior, providing additional support to the theoretical calculations presented in Ref. 4, for the entire temperature range. A $n-m$ family behavior can be observed in our experimental data (Fig. 5) for the nanotube species (7,6) and (8,7), (7,5) and (8,6), and (9,4) and (8,3). This family behavior with strain was predicted by a theoretical approach describing the behavior of carbon nanotubes under hydrostatic pressure,¹⁹ and is finally well reproduced by our theoretical fit.

In order to understand the behavior of the different nanotube species under strain, we follow the relation of the band-gap shift introduced recently by Gartstein *et al.*, Eq. (24) in Ref. 18. The band-gap change under small strains is given by

$$\begin{aligned}
 \delta E_g = & - \frac{2 \left[\frac{\eta - 1}{(\eta + 1)z_a} + 1 \right] |\gamma| a_{C-C}}{d} \varepsilon_r \\
 & + 3 |\gamma| (\varepsilon_r - \varepsilon_z) (-1)^\nu \cos(3\theta), \quad (3)
 \end{aligned}$$

where the carbon-carbon bond length $a_{C-C} = 1.42 \text{ \AA}$, the nearest-neighbor hopping matrix element $\gamma = -2.89 \text{ eV}$, and the Poisson ratio $\eta = 0.27$. Following Gartstein *et al.*,¹⁸ the factor $z_a = 1.28$ accounts for the fact that the lattice does not deform under strain as the two-dimensional elastic continuum and z_a becomes unity when the difference effectively disappears. The second term in Eq. (3) is identical to the result in Ref. 23 if the torsional component is neglected and leads to the opposite energy shift for the two $\nu = (n - m) \bmod 3$ carbon nanotube families. The first chirality independent contribution in Eq. (3) arises from the renormalization of the nearest-neighbor hopping term when the lattice expands or contracts.^{18,19,45} This contribution to the energy shift is smaller than the second term, but it becomes important for smaller chiral angle nanotubes, i.e., when θ approaches zero. ε_r and ε_z are the radial and axial strains, which are related to the radial and axial elastic constants^{46–48} C_r and C_z according to $\varepsilon_r = -A/C_r$ and $\varepsilon_z = -B/C_z$. A and B are fitting parameters, which correspond to the magnitude of the radial and axial components of the strain. We have used the expressions derived in Ref. 19 [Eqs. (1) and (2)] for the elastic constants, which are diameter dependent and both decay as $1/d$ in the large diameter limit. In fact, the cases of hydrostatic pressure and stress are conceptually identical, differing only in the signs and magnitudes of the resulting radial and axial strains.¹⁹ Using the diameter dependent elastic constants improved the theoretical fit, and as a result, no torsion was needed in the fitting process. The fitting shown in Fig. 5(b) was achieved by varying only the two fitting parameters A and B , and the best fit shown corresponds to $A = 0.4342 \text{ kbar/K}$ and $B = 0.26447 \text{ kbar/K}$. The radial pressure coefficient A for the (8,4) carbon nanotube species is 0.5071 meV/kbar , similar to pressure coefficient values calculated in Ref. 19. The expansion of the wrapping polymer with increasing temperature leads most likely to an increasing nonuniform pressure in the radial and axial directions.

In conclusion, the temperature dependence of the band gap of semiconducting carbon nanotubes was measured in from 190 K to room temperature. Small and reproducible blueshifts of the emission lines with decreasing temperature were observed, showing only a moderate chirality dependence. In addition to the energy shift, a substantial line narrowing was observed, that persisted all the way to 4.2 K. Both effects, the energy shifts and the broadening, can be attributed to the electron-phonon interaction. A simple expression used in the past to reproduce the temperature broadening of the critical points of conventional semiconductors^{28,29} has been used to fit our data, which provided important insight into the strength of the electron-phonon interactions. The effect of external strain on the band gap of carbon nanotubes induced by the expansion of the wrapping polymer was also measured. The band gap of the two $\nu=(n-m)\bmod 3$ nanotube families shifts energetically in opposite directions, in agreement with previous observations,¹⁶ and a different nanotube family behavior

with strain is observed. The band gap of carbon nanotubes with equal $(n-m)$ number shifts nearly identically, independent of the tube diameter or chirality. This strain behavior of the band gap is very well reproduced for seven carbon nanotube species using Eq. (3) and by varying the strength of the radial and axial strains.^{18,19} This theoretical model provides a tool to model and predict the effect of strain on the electronic properties of semiconducting carbon nanotubes in many applications, such as their use as biological sensors.

ACKNOWLEDGMENTS

We acknowledge the financial support of the Department of Energy Office of Science, Basic Energy Sciences, Divisions of Material Sciences under DE-AC36-83CH10093. We gratefully acknowledge Rodrigo B. Capaz for suggestions regarding the theory used to reproduce the strain shifts and for the critical reading of the paper.

*Electronic address: denis_karaiskaj@nrel.gov

- ¹C. D. Spataru, S. Ismail-Beigi, L. X. Benedict, and S. G. Louie, Phys. Rev. Lett. **92**, 077402 (2004).
- ²E. Chang, G. Bussi, A. Ruini, and E. Molinari, Phys. Rev. Lett. **92**, 196401 (2004).
- ³H. Zhao and S. Mazumdar, Phys. Rev. Lett. **93**, 157402 (2004).
- ⁴R. B. Capaz, C. D. Spataru, P. Tangney, M. L. Cohen, and S. G. Louie, Phys. Rev. Lett. **94**, 036801 (2005).
- ⁵V. Perebeinos, J. Tersoff, and P. Avouris, Phys. Rev. Lett. **94**, 027402 (2005).
- ⁶S. Roche, J. Jiang, F. Triozon, and R. Saito, Phys. Rev. Lett. **95**, 076803 (2005).
- ⁷V. Perebeinos, J. Tersoff, and P. Avouris, Phys. Rev. Lett. **94**, 086802 (2005).
- ⁸J. Jiang, R. Saito, A. Grüneis, S. G. Chou, G. G. Samsonidze, A. Jorio, G. Dresselhaus, and M. S. Dresselhaus, Phys. Rev. B **71**, 205420 (2005).
- ⁹M. Machón, S. Reich, H. Telg, J. Maultzsch, P. Ordejón, and C. Thomsen, Phys. Rev. B **71**, 035416 (2005).
- ¹⁰S. Reich, M. Dworzak, A. Hoffmann, C. Thomsen, and M. S. Strano, Phys. Rev. B **71**, 033402 (2005).
- ¹¹F. Plentz, H. B. Ribeiro, A. Jorio, M. S. Strano, and M. A. Pimenta, Phys. Rev. Lett. **95**, 247401 (2005).
- ¹²D. Karaiskaj, C. Engtrakul, T. McDonald, M. J. Heben, and A. Mascarenhas, Phys. Rev. Lett. **96**, 106805 (2006).
- ¹³S. B. Cronin, Y. Yin, A. Walsh, R. B. Capaz, A. Stolyarov, P. Tangney, M. L. Cohen, S. G. Louie, A. K. Swan, M. S. Ünlü *et al.*, Phys. Rev. Lett. **96**, 127403 (2006).
- ¹⁴J. Lefebvre, P. Finnie, and Y. Homma, Phys. Rev. B **70**, 045419 (2004).
- ¹⁵P. Finnie, Y. Homma, and J. Lefebvre, Phys. Rev. Lett. **94**, 247401 (2005).
- ¹⁶L.-J. Li, R. J. Nicholas, R. S. Deacon, and P. A. Shields, Phys. Rev. Lett. **93**, 156104 (2004).
- ¹⁷J. Wu *et al.*, Phys. Rev. Lett. **93**, 017404 (2004).
- ¹⁸Y. N. Gartstein, A. A. Zakhidov, and R. H. Baughman, Phys. Rev. B **68**, 115415 (2003).
- ¹⁹R. B. Capaz, C. D. Spataru, P. Tangney, M. L. Cohen, and S. G. Louie, Phys. Status Solidi B **241**, 3352 (2004).
- ²⁰A. G. Souza Filho, N. Kobayashi, J. Jiang, A. Grüneis, R. Saito, S. B. Cronin, J. Mendes Filho, G. G. Samsonidze, G. Dresselhaus, and M. S. Dresselhaus, Phys. Rev. Lett. **95**, 217403 (2005).
- ²¹S. M. Bachilo *et al.*, Science **298**, 2361 (2002).
- ²²M. J. O'Connell *et al.*, Science **297**, 593 (2002).
- ²³L. Yang and J. Han, Phys. Rev. Lett. **85**, 154 (2000).
- ²⁴L. Yang, M. P. Anantram, J. Han, and J. P. Lu, Phys. Rev. B **60**, 13874 (1999).
- ²⁵P. B. Allen and M. Cardona, Phys. Rev. B **23**, 1495 (1981).
- ²⁶P. B. Allen and M. Cardona, Phys. Rev. B **27**, 4760 (1983).
- ²⁷S. Gopalan, P. Lautenschlager, and M. Cardona, Phys. Rev. B **35**, 5577 (1987).
- ²⁸P. Lautenschlager, P. B. Allen, and M. Cardona, Phys. Rev. B **33**, 5501 (1986).
- ²⁹L. Viña, S. Logothetidis, and M. Cardona, Phys. Rev. B **30**, 1979 (1984).
- ³⁰H. Htoon, M. J. O'Connell, P. J. Cox, S. K. Doorn, and V. I. Klimov, Phys. Rev. Lett. **93**, 027401 (2004).
- ³¹H. Suzuura and T. Ando, Phys. Rev. B **65**, 235412 (2002).
- ³²V. N. Popov and P. Lambin, Phys. Rev. B **74**, 075415 (2006).
- ³³S. V. Goupalov, B. C. Satishkumar, and S. K. Doorn, Phys. Rev. B **73**, 115401 (2006).
- ³⁴G. Pennington and N. Goldsman, Phys. Rev. B **68**, 045426 (2003).
- ³⁵G. D. Mahan, Phys. Rev. B **68**, 125409 (2003).
- ³⁶M. Lazzeri, S. Piscanec, F. Mauri, A. C. Ferrari, and J. Robertson, Phys. Rev. Lett. **95**, 249901 (2005).
- ³⁷J. Lee, E. S. Koteles, and M. O. Vassell, Phys. Rev. B **33**, 5512 (1986).
- ³⁸V. Srinivas, J. Hryniewicz, Y. J. Chen, and C. E. C. Wood, Phys. Rev. B **46**, 10193 (1992).
- ³⁹T. Ruf, J. Spitzer, V. F. Sapega, V. I. Belitsky, M. Cardona, and K.

- Ploog, Phys. Rev. B **50**, 1792 (1994).
- ⁴⁰S. Rudin, T. L. Reinecke, and B. Segall, Phys. Rev. B **42**, 11218 (1990).
- ⁴¹S. Rudin and T. L. Reinecke, Phys. Rev. B **41**, 3017 (1990).
- ⁴²W. Braun, M. Bayer, A. Forchel, H. Zull, J. P. Reithmaier, A. I. Filin, and T. L. Reinecke, Phys. Rev. B **56**, 12096 (1997).
- ⁴³J.-Y. Park, S. Rosenblatt, Y. Yaish, V. Savonova, H. Üstünel, S. Braig, T. A. Arias, P. W. Brouwer, and P. L. McEuen, Nano Lett. **4**, 517 (2004).
- ⁴⁴T. Inoue, K. Matsuda, Y. Murakami, S. Maruyama, and Y. Kane-
mitsu, Phys. Rev. B **73**, 233401 (2006).
- ⁴⁵C. L. Kane and E. J. Mele, Phys. Rev. Lett. **93**, 197402 (2004).
- ⁴⁶S. Reich, C. Thomsen, and P. Ordejón, Phys. Rev. B **65**, 153407 (2002).
- ⁴⁷S. Reich, C. Thomsen, and P. Ordejón, Phys. Status Solidi B **235**, 354 (2003).
- ⁴⁸C. Thomsen, S. Reich, H. Jantoljak, I. Loa, K. Syassen, M. Burghard, G. S. Duesberg, and S. Roth, Appl. Phys. A: Mater. Sci. Process. **69**, 309 (1999).